

Fitness Maturation of Engineered AAV Capsid STAC-102 Enhances Central Nervous System Transduction after CSF Administration in Cynomolgus Macaques

David S. Ojala, Lori Andrews, Ankitha Nanjaraj, Matthew Tiffany, Nathan Palmer, Yuri Bendaña, Russell Darst, Stephen Wist, Alicia Goodwin, Kenneth Kennard, Sarah Mueller, Amy M. Pooler
Sangamo Therapeutics Inc., 501 Canal Blvd, Richmond, CA 94804, USA



Introduction

- The clinical translation of genomic medicines to treat disorders of the central nervous system (CNS) has been limited by inefficient gene delivery.
- AAV administration into the cerebrospinal fluid enables access to the CNS with relatively low doses and limited exposure to pre-existing anti-AAV antibodies.
- We previously applied the functional selection platform SIFTER (Selecting In vivo for Transduction and Expression of RNA) to identify capsids with improved CNS transduction after cerebrospinal fluid (CSF) administration.
- The engineered capsids STAC-102 and STAC-103 exhibited a 10- to 100-fold enrichment in both vector genome biodistribution and neuronal mRNA expression compared to AAV9 across key CNS regions.
- Here we describe the fitness maturation of capsid STAC-102 and identification of second generation STAC-102 variants that mediate an additional 5- to 10-fold increase in CNS delivery in cynomolgus macaques.

Fitness maturation of capsid STAC-102

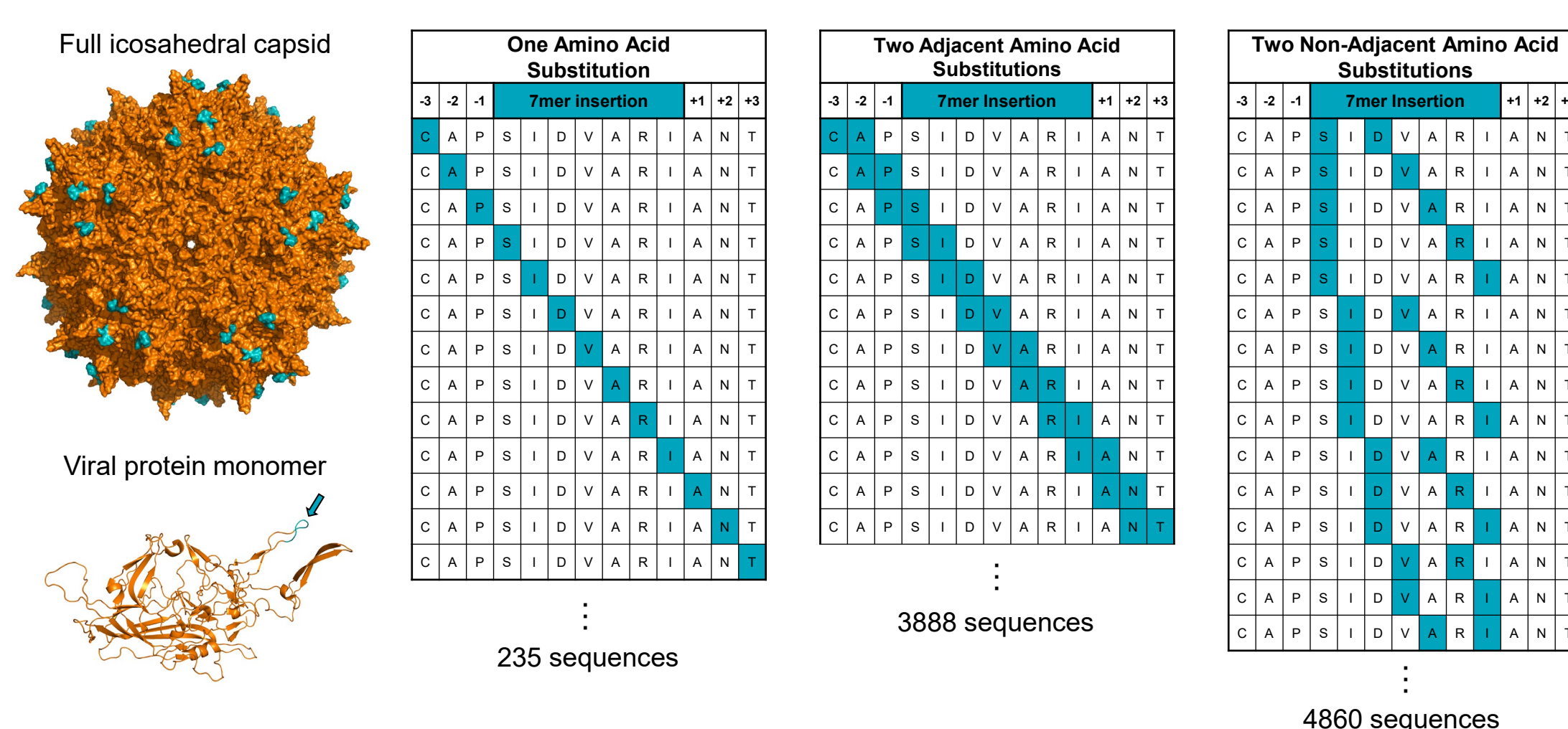


Figure 1. Fitness maturation strategy. Each mutated position was changed to all possible amino acids except cysteine and the original amino acid in STAC-102. A total of ~9000 capsid sequences were designed, and each was synthesized with three unique barcodes.

SIFTER capsid screening platform

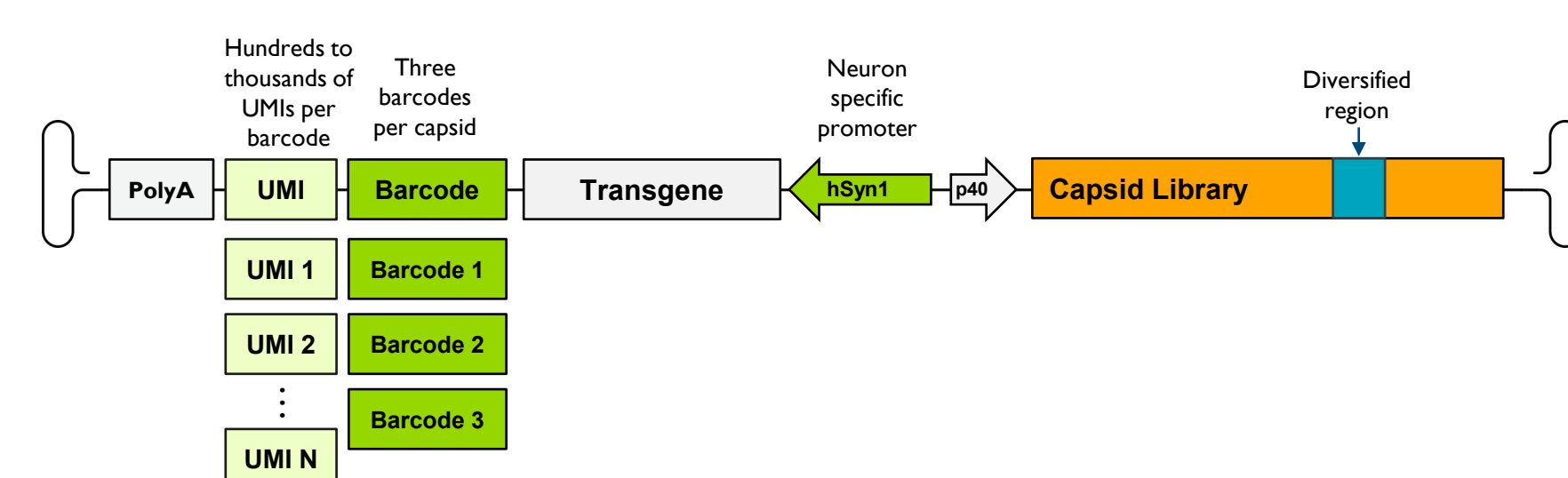


Figure 2. Library design for functional capsid selection. Each capsid is linked to three unique barcodes using a bioinformatic look-up table. Hundreds to thousands of unique molecular identifiers (UMIs) are cloned per barcode to enable greater interpretation of distinct AAV transduction events. Capsid performance is evaluated based on barcoded mRNA expression from the neuron specific hSynapsin I promoter.

HEK293 manufacturing yield

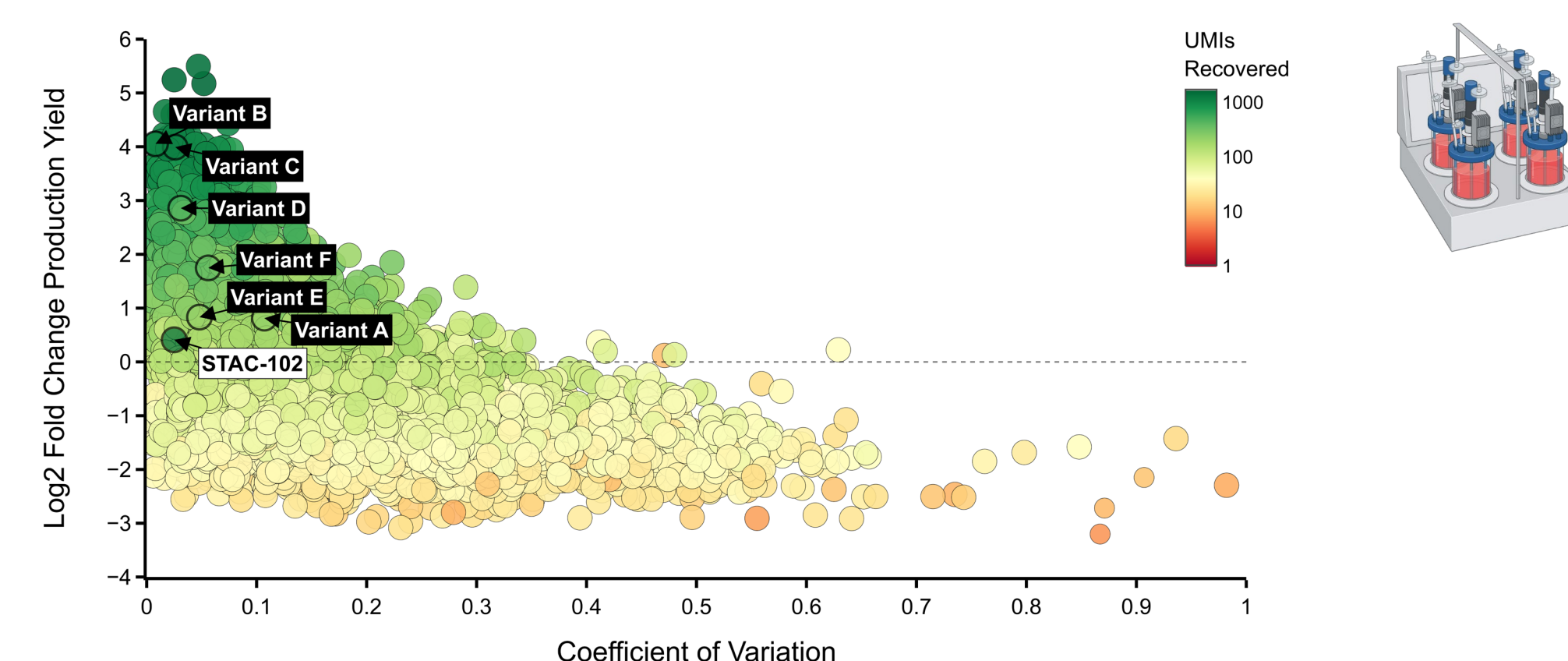


Figure 3. Library evaluation of HEK293 manufacturing yield. High performing capsids have the following features in the bubble plots:
1) High log₂ fold enrichment, these data are normalized by input abundance (y-axis)
2) Low coefficient of variation (x-axis)
3) High fraction of sequenced samples in which a capsid is found (large bubble size)
4) Robust unique molecular identifier recovery (green color)

The parent capsid STAC-102 and notable second-generation capsids with improved performance in cynomolgus macaques are annotated.

In vitro transduction in mouse and human neurons

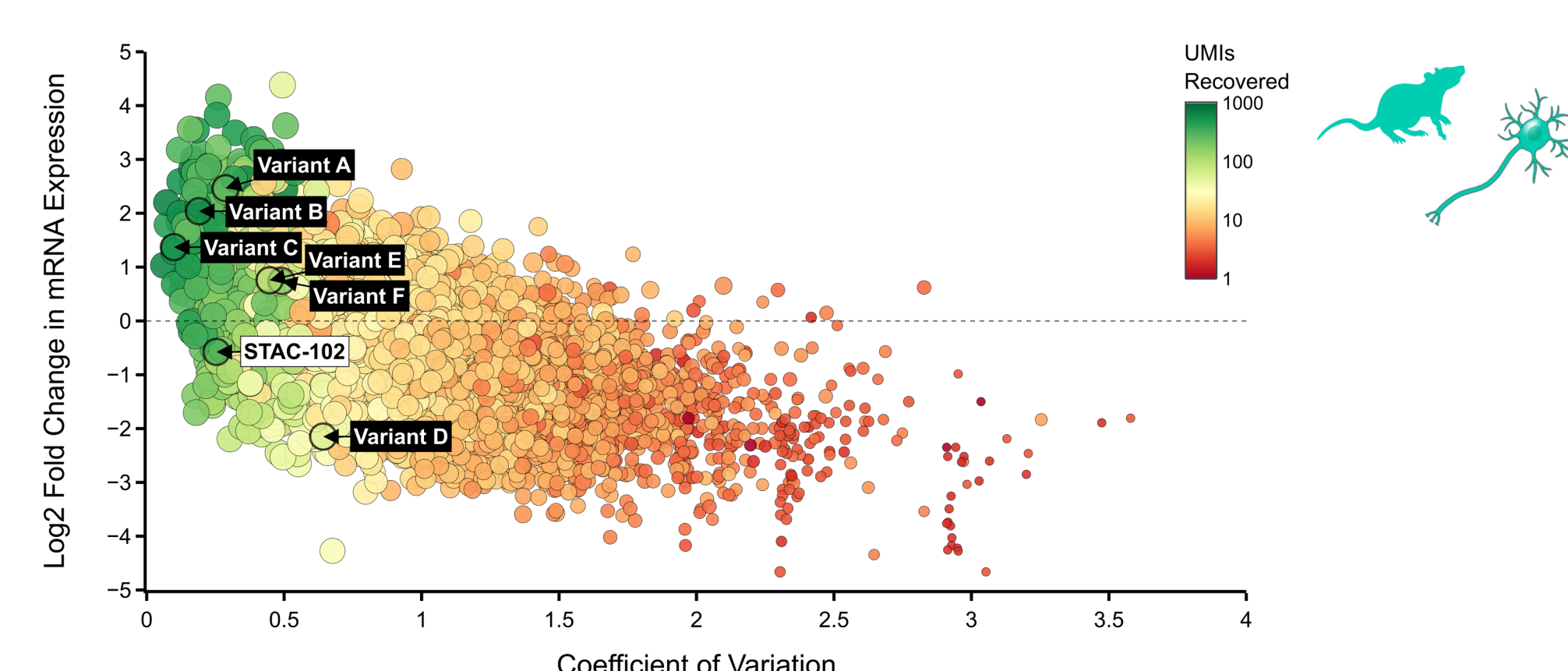


Figure 4. In vitro transduction of mouse cortical neurons. Barcode expression in neurons was assessed 5 days post-transduction. Annotated second generation variants exhibit up to an 8-fold increase in mRNA expression relative to STAC-102.

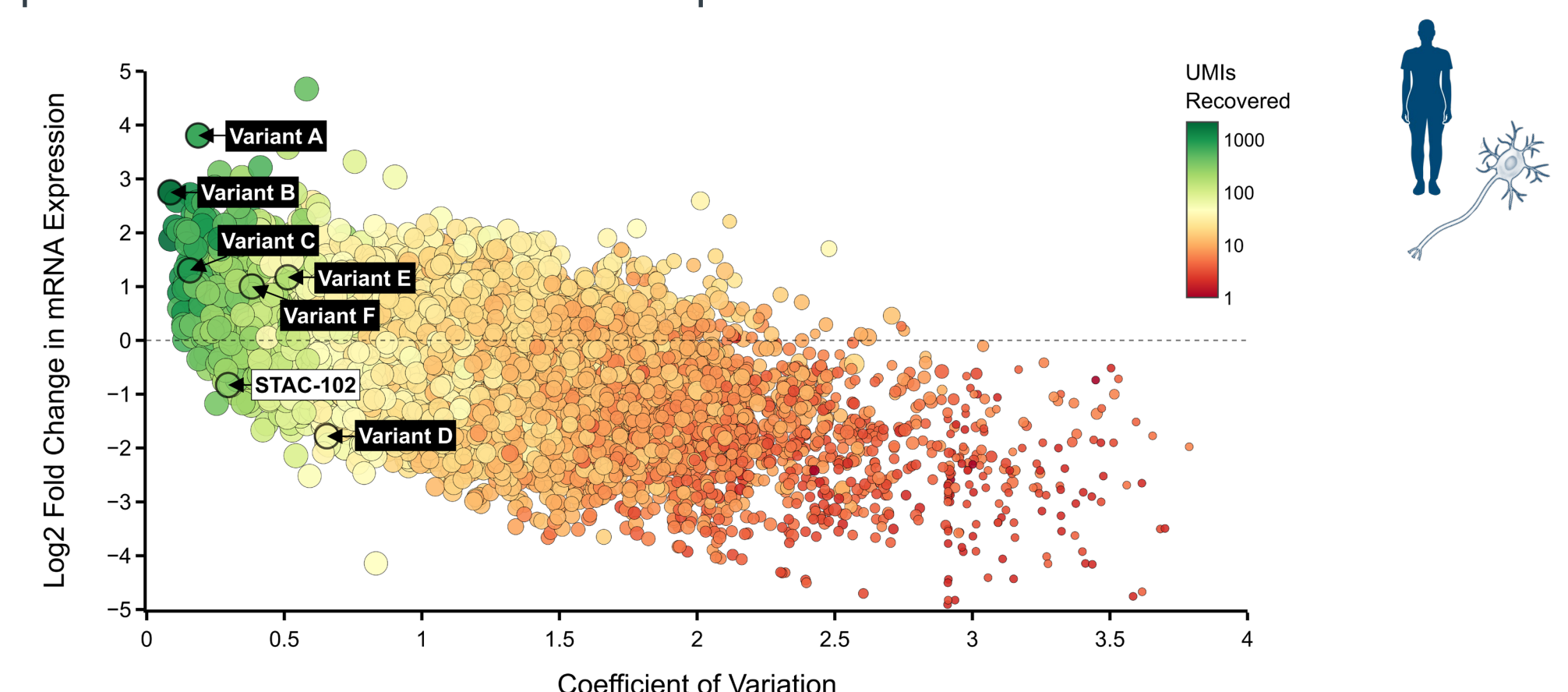


Figure 5. In vitro transduction of human iPSC-derived neurons. Barcode expression in neurons was assessed 9 days post-transduction. Annotated second generation variants exhibit up to a 25-fold increase in mRNA expression relative to STAC-102.

CNS transduction after CSF delivery in macaques

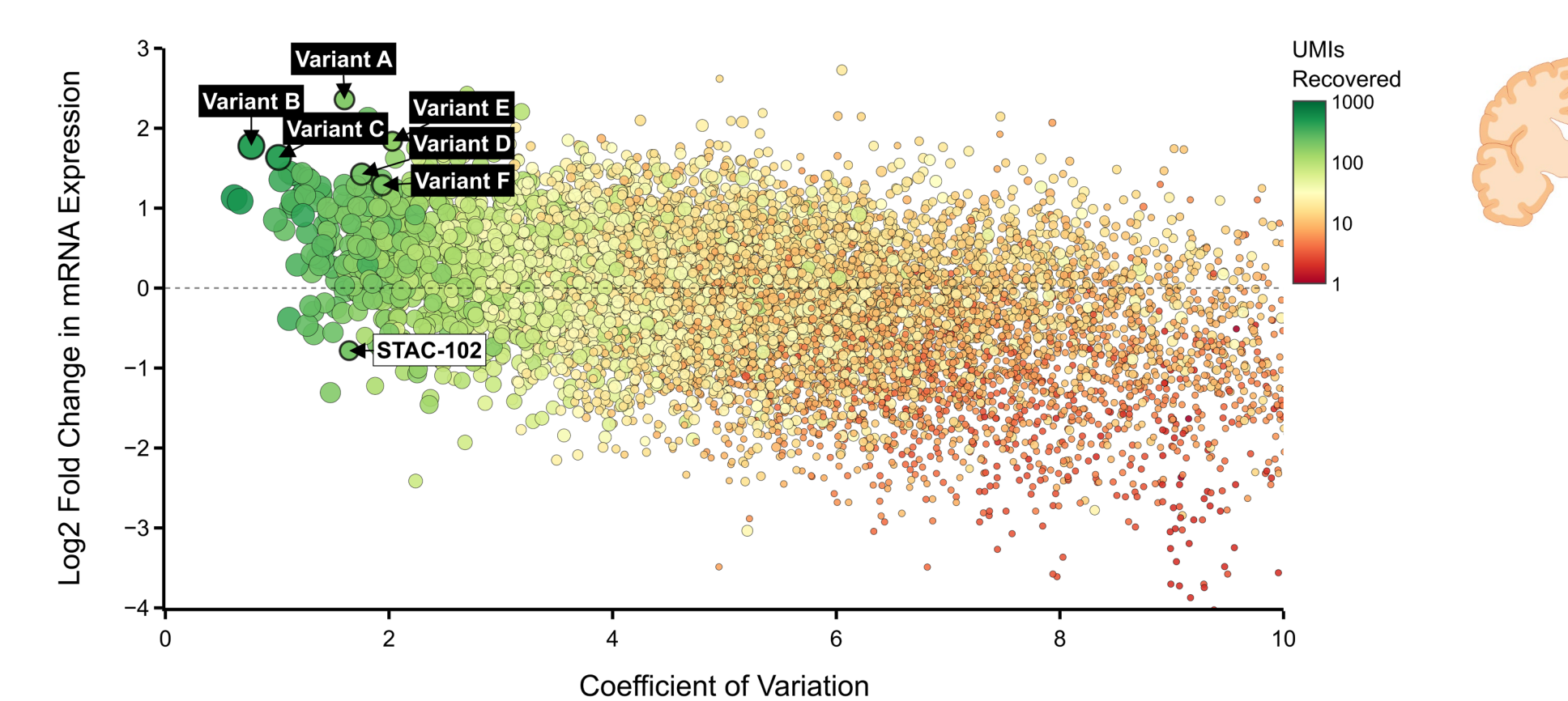


Figure 6. Neuronal mRNA expression in whole brain slices. Two coronal slices from the forebrain and hindbrain were analyzed. Annotated second generation variants exhibit up to a 9-fold increase in mRNA expression relative to STAC-102.

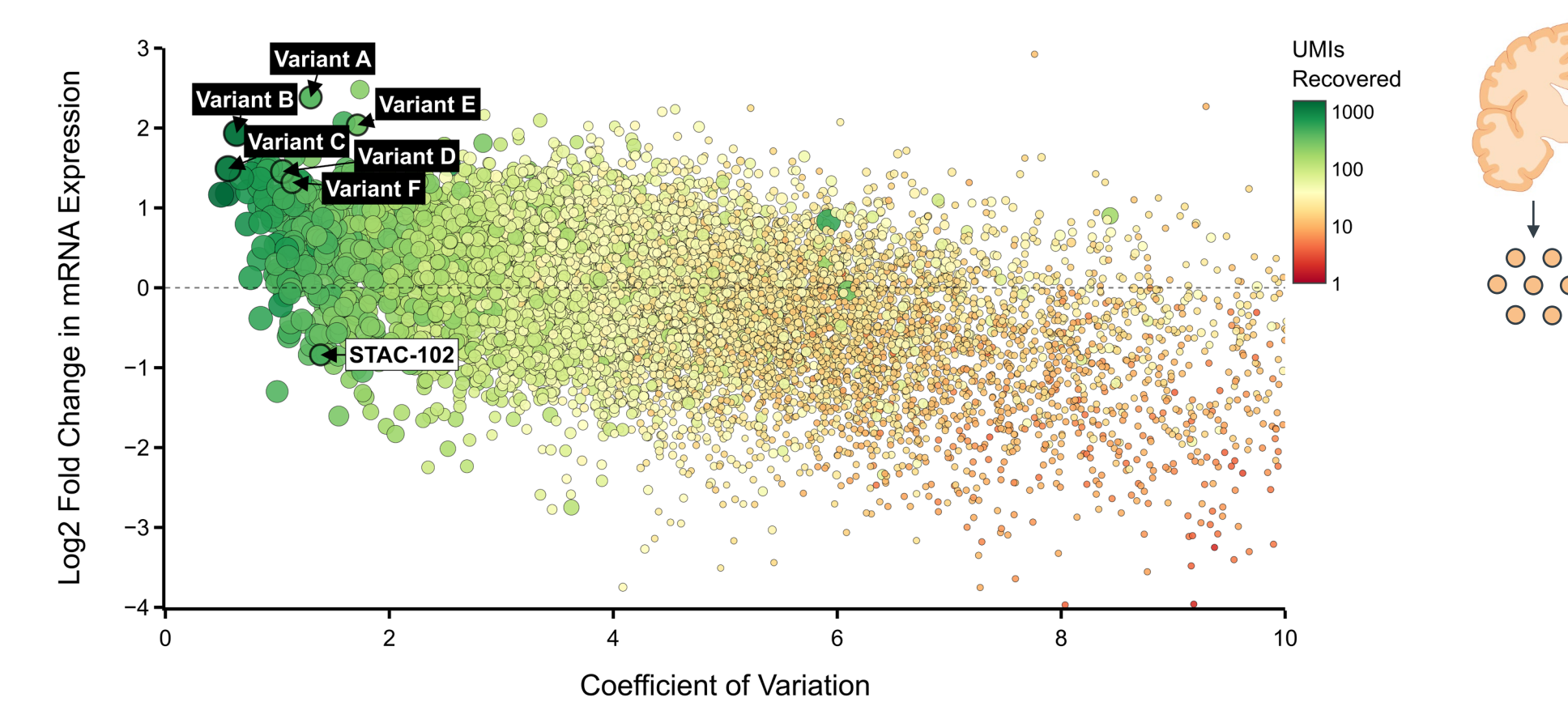


Figure 7. Neuronal mRNA expression in cortex brain punches. Brain punches were analyzed from 23 cortical regions and data were pooled. Annotated second generation variants exhibit up to a 10-fold increase in mRNA expression relative to STAC-102.

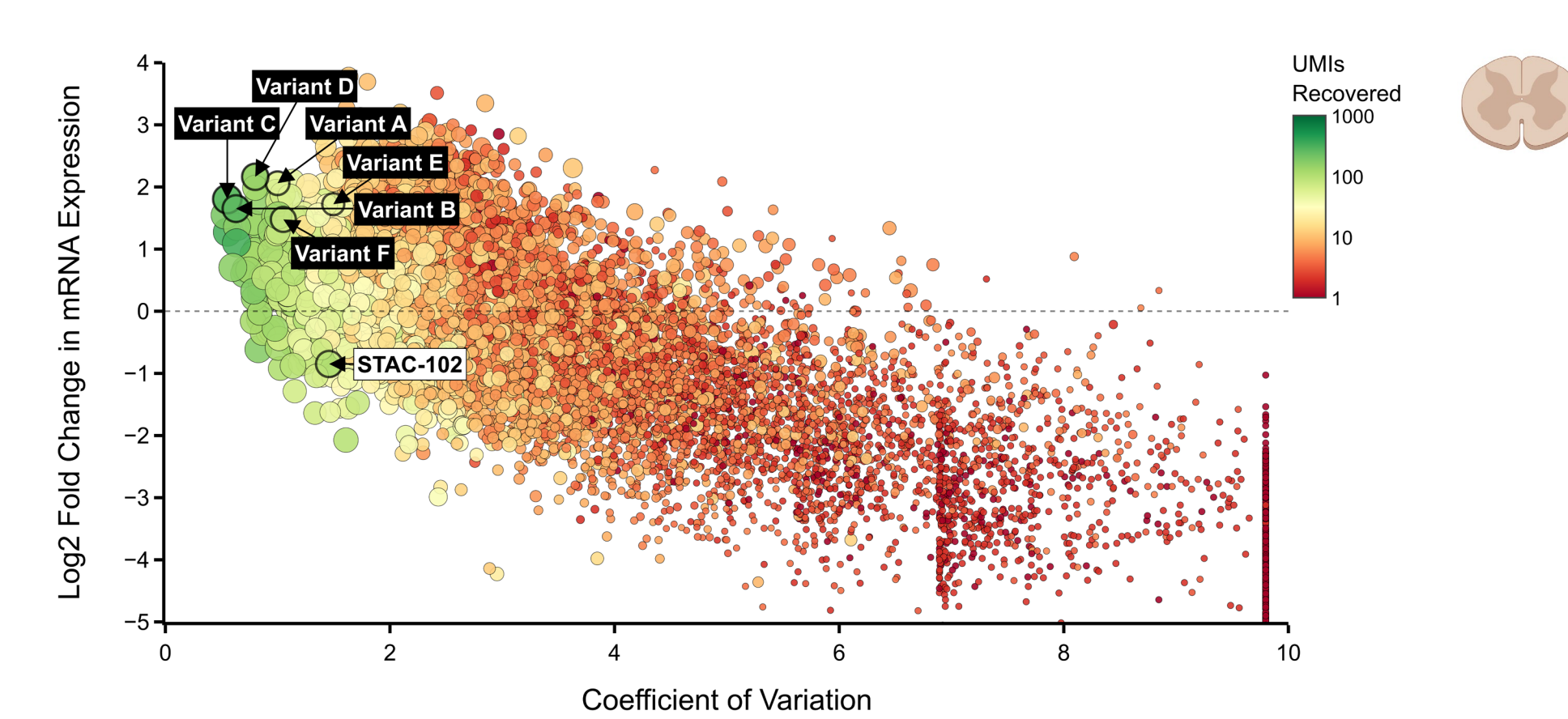


Figure 8. Neuronal mRNA expression in the spinal cord. Cervical, thoracic, and lumbar regions were analyzed. Annotated second generation variants exhibit up to an 8-fold increase in mRNA expression relative to STAC-102.

Second generation STAC-102 variants exhibit enhanced performance across multiple metrics

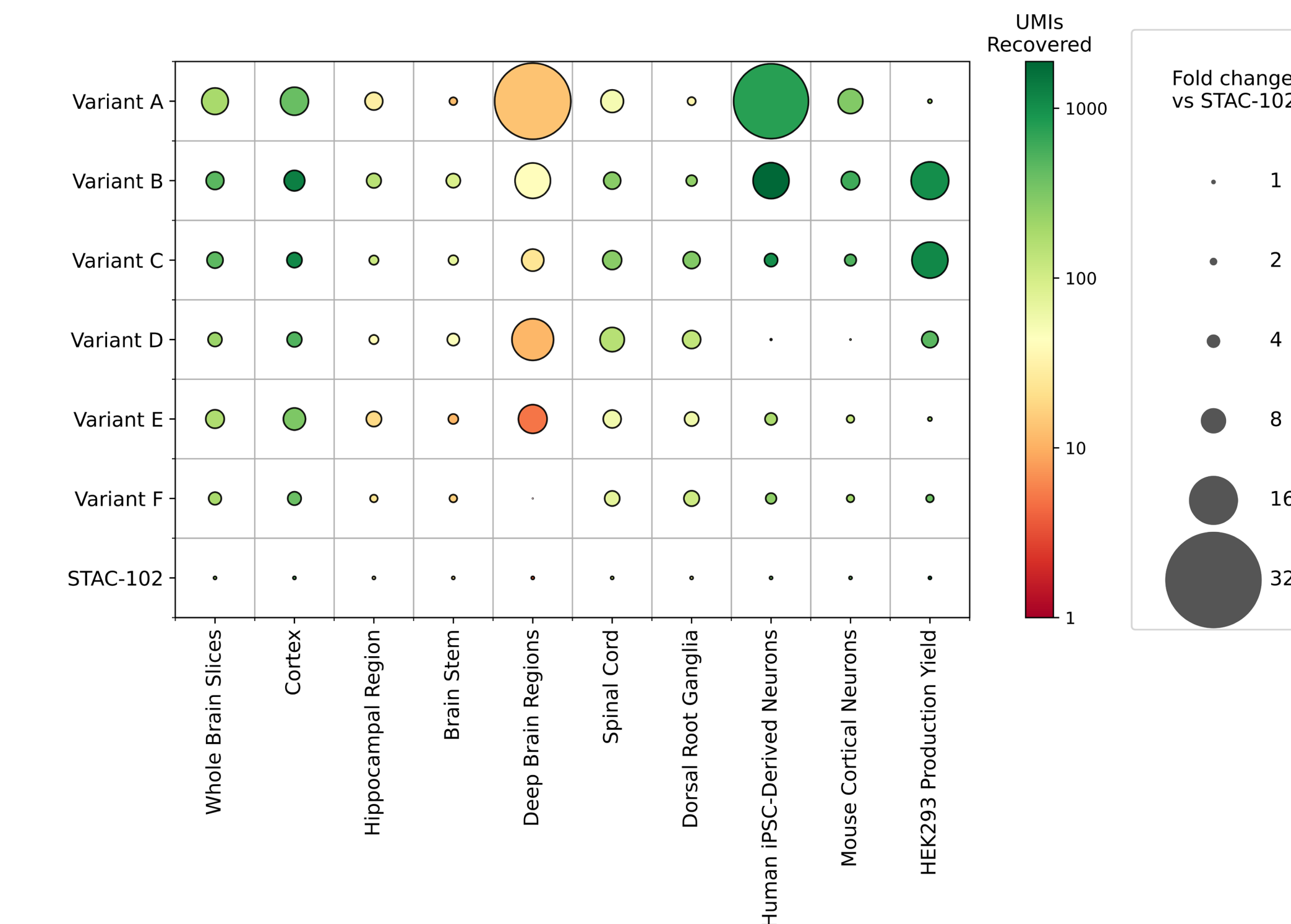


Figure 9. Summary of second generation STAC-102 capsid performance. Fold change is calculated relative to STAC-102. Bubble size is proportional to fold change and UMI recovery is indicated by color.
• Six second generation variants were chosen based on their consistently high performance in cynomolgus macaque CNS tissues and manufacturing yield that is similar or better than the parent capsid STAC-102.
• Interestingly, most of these variants likewise outperformed the STAC-102 parent in both mouse cortical neurons and human iPSC-derived neurons in vitro.
• As expected, deep brain structures that are more difficult to transduce from the ICM route show a lower number of UMIs recovered.

Conclusion

- Fitness maturation of STAC-102 identified second generation variants with 5-10x higher neuronal mRNA expression in cynomolgus macaque after CSF administration.
- Library assessment suggests that these capsids have a similar or better manufacturing yield compared to STAC-102.
- Bioinformatic analysis of fold enrichment, coefficient of variation, and UMI recovery was used to select the lead capsids.
- Second generation STAC-102 capsids will be evaluated individually in cynomolgus macaques and are promising candidates to enable therapeutics for CNS indications.

Disclosures

All authors are employees of Sangamo Therapeutics. Select figures created with BioRender.com.